THE GEOLOGICAL SOCIETY OF AMERICA®

A Late Cretaceous polygonal fault system in central North America

Andy St-Onge†
PFS Interpretations Ltd., 427 28 Avenue NW, Calgary, Alberta T2M 2K7, Canada

ABSTRACT

Polygonal fault systems (PFS) have been interpreted worldwide using seismic data imaging sedimentary strata. Normal faults initiate over a large area in fine-grained subaqueous strata soon after deposition. As they continue to grow laterally and vertically, their fault traces intersect to form polygons in plan view. These polygons are difficult to image without three-dimensional (3-D) seismic data. The faulting is initiated during sediment dewatering and mud particle consolidation that can be independent of external stresses. In the past 20 years, hundreds of basins worldwide have been interpreted to contain polygonal faults.

This paper presents a PFS interpretation for fine-grained sediments deposited in the Late Cretaceous Western Interior Seaway of the Great Plains of North America. The faulted strata have been observed as a PFS at depths ranging from ~2750 m subsurface to outcrop. Seismic dataset interpretations and borehole analyses corroborate previously published outcrop analyses and seismic interpretations. The larger observed faults are mesoscale in size, with throws up to 80 m, and strike lengths up to ~1.5 km. Potentially encompassing over 2,000,000 km^2, observational averages imply 10^7 or more mesoscale-size faults, with an order of magnitude greater number of smaller faults. At shallow depth and outcrop, the PFS model of extensive normal faulting could help to explain Late Cretaceous shale faulting attributed to other causes such as deeper sediment dissolution or glacial processes. In the subsurface, faulting and fracturing consistent with a PFS model can help to explain fault geometries observed in well control and 3-D seismic data.

INTRODUCTION

Polygonal fault systems (PFS) are geological phenomena first identified by Henriet et al. (1991) on two-dimensional (2-D) seismic data acquired at the edge of the North Sea Basin. The interpretation of over 15,000 km of 2-D seismic data resulted in the detailed mapping of fault patterns in an Eocene clay that extended to outcrop. Faults with strikes of up to 1 km, throws of up to several meters, and dips from 45° to 80° characterize the faulting, which was interpreted to have occurred shortly after mud deposition. Henriet et al. (1991) studied the observed faults in an attempt to identify the timing of the faults in the low-permeability muds and the effect they may have had on hydrocarbon migration.

The faulting in PFS is predominantly normal faulting in sediments with a large amount of fine-grained material (Dewhurst et al., 1999), and it has been shown that the faulting can occur with no external stress (Cartwright and Lonergan, 1996; Dewhurst et al., 1999). Moreover, the layer undergoing the polygonal faulting does not require net extension (Cartwright and Lonergan, 1996). PFS can occur over very large areas and can be bounded above and below by strata that are not faulted (see Cartwright and Dewhurst, 1998; see also Ostanin et al., 2012; or Watterson et al., 2000).

Syneresis is the process of the spontaneous contraction of a gel without evaporation of the solvent (Brinker and Scherer, 1990). Dewhurst et al. (1999) reported that syneresis in fine-grained sediments (considering them as gels with colloidal properties) is a key factor in the development of polygonal fault sediments Syneresis in muds can occur as a result of changing water salinities (Zhang and Buatois, 2014). Variable water salinity has been modeled for the Western Interior Seaway (Slingerland et al., 1996). These variations suggest that syneresis from water salinity variations could have initiated a PFS in the Western Interior Seaway, and this possibility is currently being investigated.

Goulty (2001) argued that low coefficients of residual friction in siliciclastic muds are the key to fault growth. Other possibilities for fault generation by volume reduction are the expulsion of biogenic gas developed in the sediments (Gay et al., 2004) or the expulsion of trapped fluid, as recently modeled using clay microphysics (Lopez et al., 2015). A large PFS with many well penetrations and outcrop, as presented here, could help to explain fluid expulsion mechanics for a PFS.

Since 1991, there have been hundreds of PFS identified throughout the world, usually identified through the interpretation of three-dimensional (3-D) seismic data (Cartwright, 2011). Most systems occur in marine basins, while only a few have been identified on land (see Tewksbury et al., 2014). The normal faults begin in relatively unconsolidated fine-grained mudstones ranging from pure smectitic claystones to almost pure chalks (Cartwright and Dewhurst, 1998). The timing of faulting has implications for hydrocarbon migration, especially if the PFS faulted before source rock generation and if the faults subsequently remained open or were closed after lithification (Ishii et al., 2010).

Findings in recent publications show an improved understanding of the origin, morphology, and geometry of these complex features. Analysis has shown that PFS geometries can be indicators of deeper stratigraphy such as porous hydrocarbon reservoirs (Jackson et al., 2014) or salt diapirs (Carruthers et al., 2013). The lateral termination of fault growth in siliceous mudstones was observed and modeled by Ishii et al. (2010). They found that fault propagation in weak mudstones similar to those found in PFS can grow by either tensile failure or shear failure, depending upon the rock strength and external stress. Further advances have been made in the evolution of PFS using geomechanical forward modeling (Roberts et al., 2015). An intriguing result of this is the potential that PFS geometries can be used as an indicator of paleostress.

Cartwright (2014) argued that understanding of PFS would be improved by integrating seismic data, outcrop analysis, and borehole

†geophysicist@shaw.ca; mast@shaw.ca

GSA Bulletin; May/June 2017; v. 129; no. 5/6; p. 582–593; doi: 10.1130/B31582.1; 11 figures; 1 table; Data Repository item 2016364; published online 23 February 2017.

logging. Recently, Tewksbury et al. (2014) reported on the discovery and interpretation of a 900 km^2 PFS in a Cretaceous chalk outcropping in Egypt. They identified outcrop features that could be important in the explanation of PFS development. The features included small circular regions that they postulated could be areas of overpressured fluid expulsion.

Maher et al. (2015) reported on the examination of an outcrop of the Late Cretaceous Pierre Shale in South Dakota. The strata-bound vein array continues unabated in a 2–4-m-thick interval over a 50-km-long outcrop. They noted that the vein array has uniform horizontal extension and surmised that it could be caused by diagenetically driven deformation in the subsurface. It is argued here that the vein array is part of a regional-scale PFS.

In this paper, I report observations consistent with the occurrence of a PFS beneath the Great Plains of North America. This report presents evidence for the PFS but does not discuss the particular mechanism for the PFS formation, which requires much more analysis. The extent of the Great Plains PFS is still being mapped, but it could be on the order of 2,000,000 km^2 or more. The size of the PFS could be similar to the Upper Cretaceous PFS in the Eromanga Basin in Australia (Cartwright, 2011). The PFS boundaries range from southeast Alberta to southwest Manitoba in Canada and extend south into northeast Colorado and western Kansas, United States. The PFS has been sampled by over 300,000 wellbores, mapped in outcrop (Maher et al., 2015), and imaged with 3-D seismic data (Sonnenberg and Underwood, 2012). Evidence for this study is provided by the interpretation of numerous 3-D seismic datasets, and wellbore and outcrop analysis in Alberta, Saskatchewan, and Manitoba. The fault extents, offsets, and geometry are consistent with the identification of PFS in the past 25 yr, supporting a PFS model for the Late Cretaceous sediments beneath the Great Plains.

The ramifications for the identification of this PFS are significant. Fracturing of the Pierre Shale would be recognized as pervasive, requiring no further geological processes. Slumping of the Pierre Shale at or near outcrop could be better understood if some of the slumping occurs at weak fault planes existing within the PFS. The PFS is a viable explanation for some unexpected surface faulting such as those observed at outcrop in Manitoba or bed faulting at open pit mines in Saskatchewan. Identification of fault blocks in an area could help to drill deep-water wells in arid regions or explain shallow biogenic gas production variations caused by permeability variations.

GEOLOGIC FRAMEWORK

Polygonal Fault Systems

PFS are extensive sets of normal faults with a 3-D geometry. They are generally formed in fine-grained depositional environments (Cartwright and Dewhurst, 1998). Vast numbers of small (<100 m of vertical throw) normal faults occur in these systems. The faults grow laterally in size until they coalesce and form polygonal outlines. In map view, PFS appear as concatenated polygons. The polygons can be amorphous or regular, as presented here. The complicated geometries are best imaged with 3-D seismic data, which have only been recorded in the past 30 yr.

PFS can range in size from ~1000 km^2 to ~2,000,000 km^2 (Cartwright, 2011). Even though PFS can cover very large areas, individual fault block geometries can remain consistent throughout the system (Watterson et al., 2000). The faults are usually concentrated in specific stratigraphic units of very fine-grained mudstones such as smectite-rich claystones, biosiliceous mudstones, and nanofossil chalks (Goulty and Swarbrick, 2005; Roberts et al., 2015). A model presently being examined using the data for this analysis is the cessation of the PFS if there is a lateral transition to sediments with clasts. Most PFS are bounded above and below by zones with no observable deformation (Cartwright and Dewhurst, 1998).

Geological Setting and Stratigraphic Context

The mid- to Late Cretaceous Western Interior Seaway covered most of central North America during much of the Mesozoic (Fig. 1). Blakey (2014) summarized the paleotectonics of the Western Interior Seaway. A retro-arc foreland basin was defined by Cordilleran subduction to the west and volcanism from the Middle

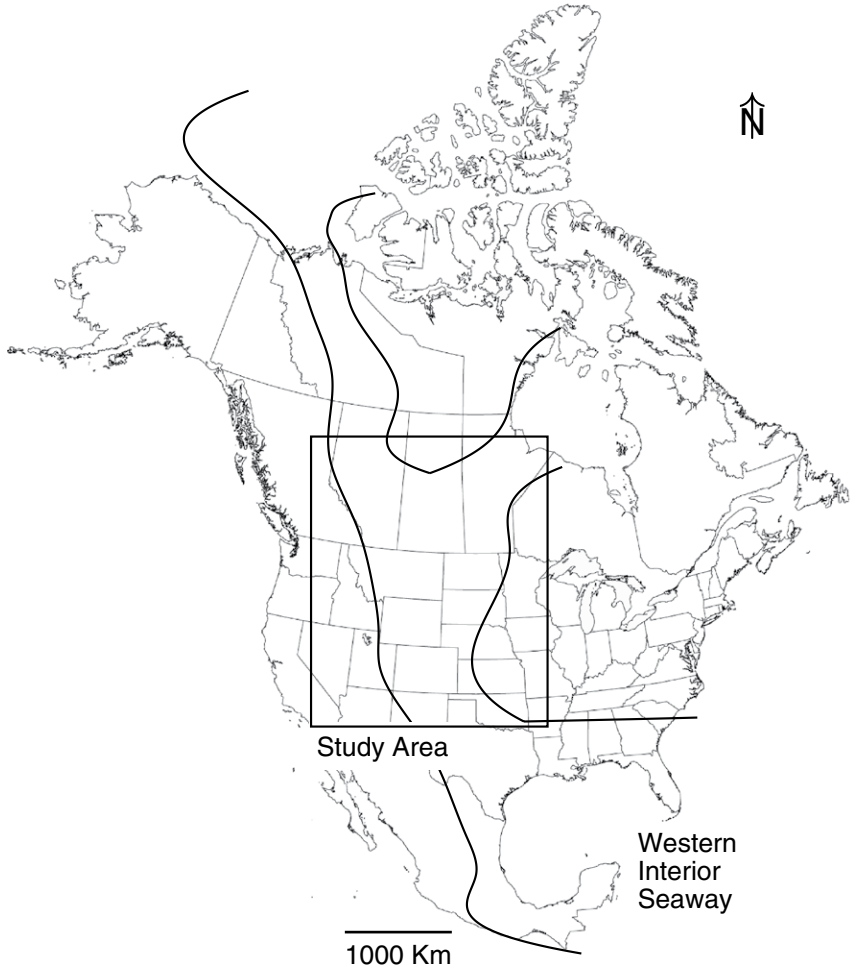

Figure 1. Map of North America showing the extent of the Western Interior Seaway during Coniacian time (Blakey, 2014).

Jurassic to Coniacian. From the Santonian to Maastrichtian, the subsidence and sedimentation patterns changed in response to shallowing subduction angles and subduction of a thick oceanic slab. This subduction caused regional uplift that partitioned the Western Interior Basin into Laramide uplifts and basins that eventually caused the withdrawal of the Western Interior Seaway.

The Late Cretaceous rocks were deposited in a single large sedimentary basin over 100 km wide extending from the Gulf of Mexico to the Arctic Ocean (Weimer, 1960). The western margin of the basin was bounded by highlands produced by the mid-Cretaceous Sevier orogeny, while the eastern margin was relatively stable cratonic lowland (Bertog, 2010). Fine-grained sediments were deposited in the Cenomanian and the Campanian interval during rising and falling sea levels (Schröder-Adams et al., 2001). The Western Interior Seaway defines a depositional limit for the occurrence of the Late Cretaceous polygonal fault system in middle North America.

Figure 2 shows the extent of the Campanian Pierre Shale as defined by outcrop edges. The area covers ~2,600,000 km^2. A large part of the outcrop is covered by a thin veneer of glacial till and dirt (Roberts and Kirschbaum, 1995). The reader is referred to Schultz et al. (1980) for a detailed description of the composition and properties of the Pierre Shale. Their work on the eastern edge of the area in Figure 2 described almost exclusively fine-grained mudstone and marlstone. Over half of 1350 analyzed samples were clay minerals.

Fine-grained strata are observed at a number of sites throughout the study area, as indicated on Figure 2. For example, Bamburak and Nicolas (2010) noted bentonitic silt and clay, siliceous shale, noncalcareous black shale with numerous bentonitic interbeds, and ferruginous black shales. There are bentonite mines at a number of locations, as shown on Figure 2. Figure 3 shows an outcrop of the Campanian Pierre Shale Odanah beds in Manitoba, Canada. Christopher et al. (2006) described 400-m-thick sequences of black shale and marlstone for the Cenomanian–Santonian Colorado Group in Saskatchewan. Gill and Cobban (1965) described Pierre Shale bentonite, organic-rich shale, chalk, and marlstone in North Dakota. Stoffer (2003) described the general shale stratigraphy of the Pierre Shale for Badlands National Park in South Dakota. The 350 m vertical section of Late Cretaceous silt clay outcrop in the South Saskatchewan River valley was described by Caldwell (1968). Maher (2014) examined the fine-grained Niobrara Chalk and Pierre Shale strata in portions of Nebraska and Kansas. Dyman et al. (1994) detailed the siliciclastic Upper Cretaceous section from southwestern Montana (exceeding 6100 m in thickness) to eastern South Dakota (~600 m thick). The salient point is that thick sections of fine-grained sediments have been detailed by others; these areas have the potential to host a PFS.

SEISMIC DATA

Datasets and Preliminary Interpretation

The dataset for this work consists of 64 3-D seismic datasets ranging in size from 3 to 100 km^2 located within the outline shown on Figure 2. All of these datasets were acquired to image oil and gas reservoirs ranging from 800 to 3200 m depth. The high signal-to-noise ratio (S:N) seismic data presented here are typical for the almost 3000 km^2 of 3-D seismic data and ~4000 line km of 2-D seismic data. The data were recorded using vertical component geophones and either dynamite or Vibroseis sources and were processed to enhance P-wave energy. Most datasets were processed to a final stacked dataset, and a poststack time-migration algorithm was applied. Precise locations for the seismic surveys are not shown on Figure 2 to respect the privacy of the data owners.

The highest-frequency datasets had a dominant frequency of ~80 Hz using the average interval velocity of ~2000 m/s in the Late Cretaceous; this implies a Fresnel zone λ/4 vertical resolution of ~6 m and a detection threshold of ~1 m. However, due to the low fold of the shallow data (and the accompanying decrease in S:N ratio), these numbers could be optimistic.

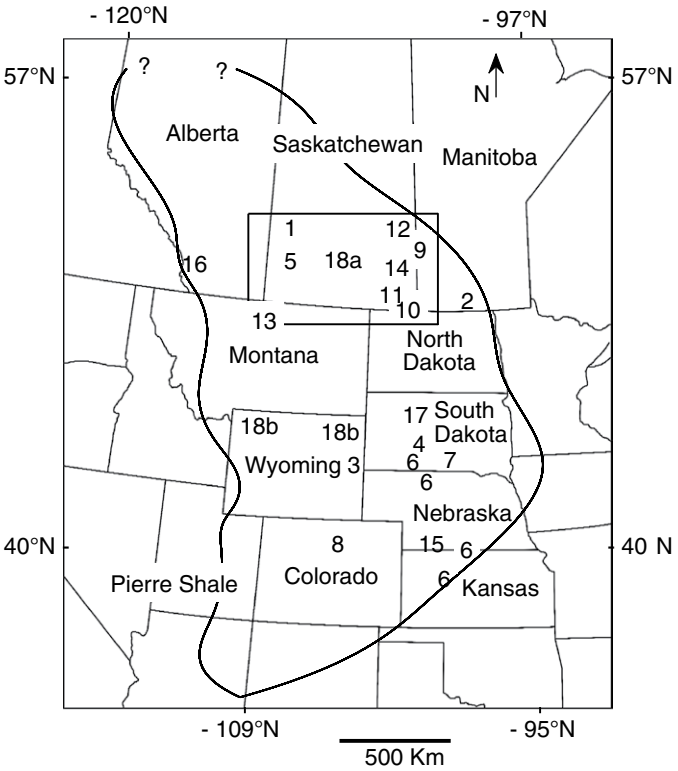

Figure 2. Outcrop edge of the Late Cretaceous Pierre Shale (modified from Roberts and Kirschbaum, 1995). Areas: 1—outline of two-dimensional (2-D) and three-dimensional (3-D) seismic dataset; 2—Manitoba field trip by Bamburak and Nicolas (2010); 3—Wyoming mapping by Gill and Cobban (1965), and Valley City, North Dakota, 46.92°N, 98.00°W; 4—Badlands National Park, South Dakota, mapping, by Stoffer (2003), 43.85°N, 102.34°W; 5—Late Cretaceous outcrop, South Saskatchewan River (Caldwell, 1968); 6—surface geology (Maher, 2014); 7—strata-bound vein array (Maher et al., 2015), Lake Francis Case, 43.24°N, 98.96°W; 8—Denver Basin (Sonnenberg and Underwood, 2015), White Rocks Outcrop, 40.05349°N, 102.013384°W; 9—Figure 4 dataset (confidential location, data courtesy of TORC Oil and Gas Ltd.); 10—Figure 7 dataset (data courtesy of TORC Oil and Gas Ltd.), 49.065482°N, 101.977875°W; 11—Figure 10 dataset (data courtesy of TORC Oil and Gas Ltd.), 49.26801°N, 103.49740°W; 13—Tiger Ridge Field (Inks, 2010), 48.402592°N, 109.421461°W; 14—Gendzwill and Stauffer (2007), 51.960620°N, 105.896587°W; 15—Harlan County Lake, Nebraska, 40.06°N, 99.29°W; 16—Lundbreck Falls, Alberta (Stockmal, 2004), 49.586961°N, 109.421461°W; 17—Teepee Buttes (Bishop and Williams, 2000), Colorado (38.599482°N, 104.643058°W), North Dakota (46.402591°N, 102.748300°W); 18—Bentonite Mines; 18a—Canadian Clay Products, 50.091345°N, 104.718187W; 18b—Bentonite Proformance Minerals, 44.837453°N, 108.389561°W.

Figure 3. Outcrop of Campanian Odanah Shale in Manitoba. Person for scale. The subvertical fault has ~0.75 m offset. Photograph courtesy of James Bamburak, Manitoba Geological Survey.

The shallow data quality was marginal on some of the datasets. Low-frequency ground roll caused by waves trapped in the low-velocity dirt and glacial till at the surface deteriorated the data quality on some datasets. This effect can be mitigated with band-pass filtering or data stacking. However, the fold at the PFS depths of 700 m or less was nominal. The densest acquisition geometry was a 3-D dataset with a source line spacing of 200 m and a receiver line spacing of 150 m (and shotpoint and geophone group intervals of 50 m). These acquisition geometries resulted in single fold coverage at 200 m, four fold coverage at 400 m depth, and nine fold coverage at 600 m depth (four fold means that one stacked seismic data trace is the combination of four data traces acquired in the field). With less-dense acquisition geometry, there are gaps in the data that extend below the PFS anomalies.

On the shallow seismic data with single or marginal fold data, high-frequency noise was not minimized by the stacking process. The shallow seismic data reflections were enhanced on numerous datasets by applying a band-pass filter or an automatic gain control (AGC) filter, or both. The typical band-pass filter applied was 8/15–65/80 Hz. The application of a single exponential gain on some of the datasets muted shallow reflection amplitudes and exaggerated the Turonian Second White Specked (2WS) reflection amplitudes as compared to synthetics traces from sonic logs. In these instances, the application of a 200 ms AGC filter was used to enhance reflection from the low-impedance contrasts for the Late Cretaceous beds.

The phases of the data were determined by using sonic and bulk density logs (if available) to construct a least squares estimate of the wavelet at the well tie point. The data were then phase rotated so that a positive impedance contrast (i.e., low to high velocity with increasing depth) was displayed as a peak reflection. The event horizons were interpreted by using geological structural values at the well locations with digital sonic logs, with small (1–2 m) adjustments for consistency in the tops picking. In the event the wellbores were not logged at depths above the wellbore surface casing, the Saskatchewan well water database was used where possible for event horizons (www.wsask.ca).

PFS Identification on 2-D and 3-D Seismic Data

All of the seismic data were interpreted by first identifying the Turonian 2WS geological marker (Favel [Assiniboine] in Manitoba and Greenhorn in the United States), a very consistent marker bed and seismic reflection that occurs through western Canada and the central United States. If any faulting was recognized at the Turonian 2WS level, a deeper Lower Cretaceous horizon, parallel to the 2WS, was also interpreted. Some faulting at and below the 2WS shale reflection event was noted at numerous locations throughout the study area. However, the Turonian 2WS reflections discussed here did not have deeper faulting observed on the data.

To identify PFS anomalies on the datasets at times earlier that the 2WS arrival time, the 3-D datasets were "time sliced" from the 2WS reflection to the earliest reflections. For this study, a time slice was an extracted seismic amplitude map at a constant time interval above or below an interpreted horizon. The amplitudes of the seismic data volumes were extracted at successive time intervals above the 2WS reflection and mapped. The time slice amplitude maps were viewed, and those with geometric anomalies were flagged for further investigation. Further investigation involved mapping consistent reflections close to the time slice; Figure 4 is an example of the result of this procedure.

Figures 4–6 show polygonal fault anomalies from a dataset in southeast Saskatchewan near the Manitoba border. The anomalies have a "mud crack" appearance when the two-way traveltimes or peak amplitudes for the Santonian Colorado reflection are displayed. The mud crack appearance covers an area of roughly 500 km^2, as shown in Figure 2. The faulting is obvious on the seismic line (Fig. 6) for an interval that extends from the interpreted Colorado reflection to ~50 ms (~50 m) above the reflection. The fault throw is 15 m ± 3 m, with dips ranging from 22° to 80°. No strike lengths were estimated for these curvilinear fault geometries. It is obvious that the faults have grown laterally and have intersected other fault traces to form a connected polygonal pattern. There were no interpretable reflections above 300 ms in this area, either due to low fold of the data or the lack of impedance contrasts in the predominantly shale strata. No surface expression of the faulted areas was observed due to surficial cover of glacial till and other Quaternary cover.

Figures 7 and 8 are a map and a seismic line showing the shallow data interpretation for a second dataset in southeast Saskatchewan. The interpretation was chosen to exemplify a representative example of connected polygonal faults at the Coniacian Govenlock interval. The structuring here shows the extensive normal faulting in the Coniacian Govenlock interval. The faulting has formed narrow (~100-m-wide) interconnected grabens. On average, 7 m of throw is observed on either side of the grabens that have an almost random strike direction. This faulting is observed on other datasets throughout southeast Saskatchewan, as

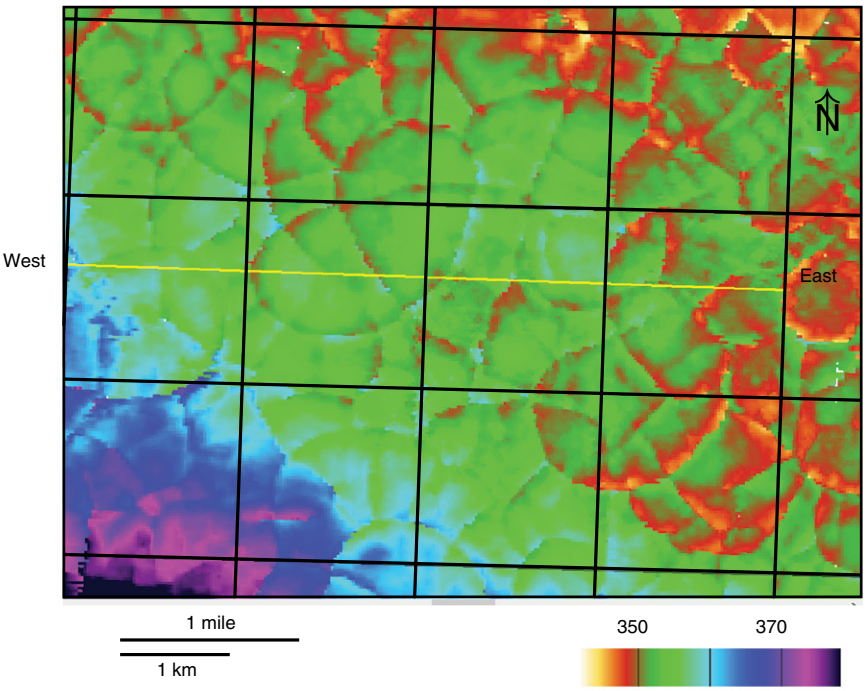

Figure 4. Map showing the Santonian Colorado two-way traveltime for a 13.1 mi² (34 km²) portion of an ~100 mi² (260 km²) 3-D seismic dataset acquired on the Saskatchewan-Manitoba border, ~160 km north of the United States. Note: 1 ms ~1 m (since V_{INT} ~2000 m/s from surface).

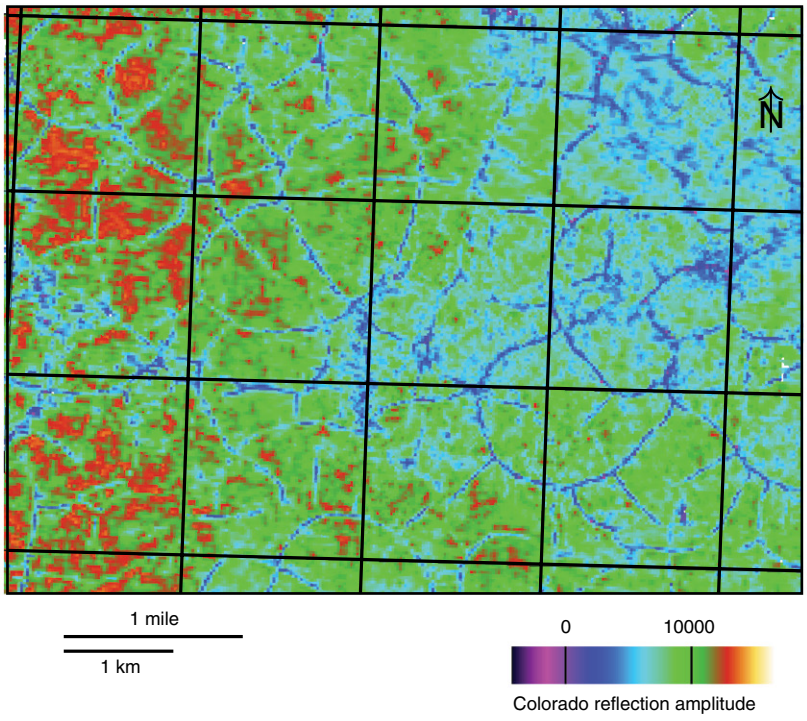

Figure 5. Map showing the Santonian Colorado reflection amplitude map for the data shown in Figure 4. The amplitudes have not been smoothed. Generally, the fault traces are low-amplitude events.

exemplified by a dataset interpretation presented at the 2016 Geological Society of America Annual Meeting (St-Onge, 2016; supplementary Powerpoint P1[1]).

Figures 9 and 10 show a PFS imaged on a 3-D dataset acquired ~150 km southwest of the area shown in Figures 4 and 5. The south edge of this dataset is ~2 km north of the Canada-U.S. border. On this dataset, there is virtually no faulting from the Turonian 2WS to the Campanian Lea Park. However, the total vertical relief of the Campanian Lea Park reflection is greater than 60 m. The S:N ratio deteriorates on the data above the Lea Park reflection and can be seen on the image as a lack of reflection signal strength.

The strike lengths for the faults averaged 900 m, and the strike throws were 30 m ± 15 m. Thirty-two strike directions were measured for the grabens on the dataset, and the preferred NE quadrant directions are shown on Figure 9. Note the complexity of the faulting on the display and the fact that many areas have structural highs and lows that are not sampled by the well control. No surface expression of the faulted areas was observed. It is believed that the unconformable Tertiary sediments (up to 100 m thick in the area) eroded Upper Cretaceous sediments that would have defined an upper bound in the tier.

The two-well cross section on Figure 11 shows that the two wells (plotted on the seismic line in Fig. 10) have ~40 m of structural offset at the Coniacian Lea Park strata within the Pierre Shale. The highly correlative beds easily show the lateral thickness changes in the sediments.

Table 1 summarizes salient PFS characteristics of the data shown here, as well as other datasets used in this study. The three datasets presented here were chosen because of the high-quality images produced for the Coniacian (Fig. 7), Santonian (Fig. 4), and the Campanian (Fig. 9). These datasets were also chosen because of their geographic range. The supplementary Powerpoint P1 (see footnote 1) presents these images for one 3-D dataset from southeast Saskatchewan and indicates how each level of the PFS appears interrelated only by faults that can persist through different ages of strata.

[1]GSA Data Repository item 2016364, supplementary Powerpoint P1, interpretation of the Great Plains polygonal fault system at Alida, Saskatchewan, presented at the 2016 Geological Society of America Annual Meeting, Denver, Colorado, September 2016, is available at http://www.geosociety.org/pubs/ft2016.htm or by request to editing@geosociety.org.

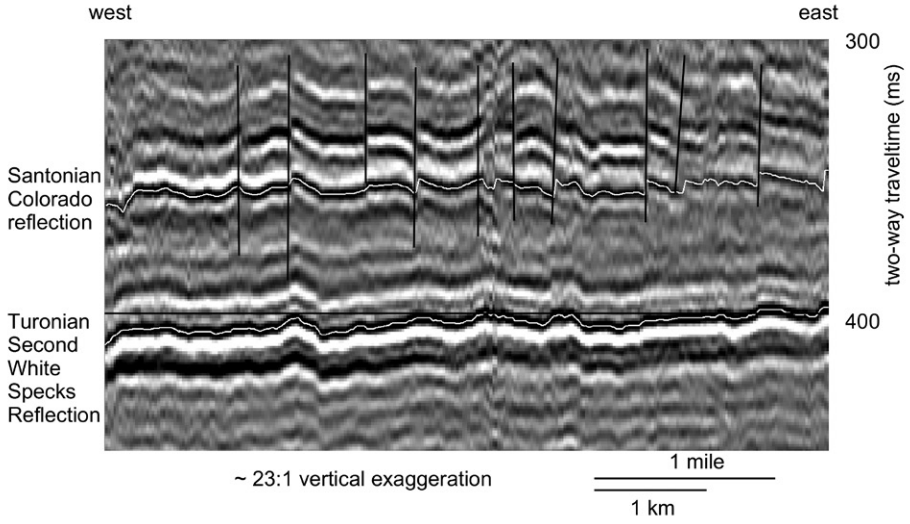

Figure 6. A 6.4 km (4 mile) west to east seismic line from the dataset shown in Figures 4 and 5. The faults dip at ~80°. Note the lack of faulting below the Turonian 2WS reflection. The vertical exaggeration is ~23:1.

SUPPORTING OBSERVATIONS BY OTHERS

Seismic Data

Several studies have presented seismic interpretations of Late Cretaceous faulting in the study area. These studies help to corroborate the presence of a continuous PFS. The studies are briefly summarized here followed by a statement about the way in which faulting from a PFS is confirmed by the example and the way in which a PFS model would change the interpretation.

Inks et al. (2010) reported on the utility of imaging the Tiger Ridge Field in Montana with 3-D seismic data (see Fig. 2). The field has produced natural gas out of the Campanian Eagle Sandstone since its discovery in 1966. The area has been interpreted as rotational fault blocks (each ~35 acres [0.14 km^2] in size) that initiated during the Eocene Bearpaw uplift, which caused the faulting. Subsequently, gravity sliding placed the fault blocks in their current location. Inks et al. (2010) noted that the individual fault blocks have independent accumulations, meaning that some faults are laterally sealing. A PFS interpretation would simply modify the interpretation made by Inks et al. (2010) to recognize that the faulting did not occur with the Bearpaw uplift, and, in fact, occurred in situ.

Gendzwill and Stauffer (2006) presented seismic and geological data from central Saskatchewan that imaged shallow Cretaceous clinoform beds and faulting imaged on 2-D seismic data. They attributed the faulting to Tertiary to Quaternary extensional tectonics or the melting of gas hydrates. A PFS interpretation would mean that this faulting could have occurred shortly after deposition.

Miller and Steeples (1996) presented 2-D seismic data acquired at Harlan County Lake, Nebraska. Recorded to image a slumping Pierre Shale fault adjacent to the dam impoundment lake, faults with up to 50 m throw within 50 m of surface were mapped. The faults have dips of 35° to 70° in a random strike pattern. All of these observed characteristics are consistent with a PFS interpretation for the faulting.

Sonnenberg and Underwood (2012) identified a PFS in the Niobrara Formation (Coniacian to Campanian) in the Denver Basin. They noted that the PFS is detached from basement faults, occurring in the Niobrara and lower Pierre Shale. The faults are minor extensional faults, randomly oriented, and they form polygonal networks in map view. The measured fault dips of 30° to 80°, throws of 9–12 m, and lengths up to 1200 m are consistent with PFS anomalies. It is thought that the Denver Basin is the deepest known part of the Late Cretaceous PFS, at depths of 2750 m.

Geological Data

Maher (2014) discussed normal faults observed in the Santonian Niobrara Chalk and Campanian Pierre Shale at locations in South Dakota, Kansas, and Wyoming (see Fig. 4). This ground-breaking work identified an easily accessible PFS outcrop (the suggestion of the name Great Plains PFS comes from the title of this paper). The faults are relatively small-scale normal faults at outcrop (up to 20 m at the Harlan Lake reservoir, for example) with a near-random strike distribution. The observations detail faulting and fracturing at a centimeter scale that simply cannot be detailed with seismic data. Maher's (2014) interpretation is that the outcrop observations are consistent with the identification of a PFS in the Denver/Julesburg Basin to the west.

Maher et al. (2015) presented results of mapping of a 50 km Pierre Shale outcrop at Lake Francis Case in South Dakota. They reported a strata-bound vein array in fine-grained mudstones along the outcrop. The veins are characterized by uniform horizontal extension. The authors observed that the outcrop has characteristics consistent with PFS, such as the strata-bound faulting in fine-grained mudstones. However, they also noted that their observations could have been caused by uniform horizontal elongation of a tectonic origin. Further surface geology and shallow seismic data imaging on the Great Plains could help to determine if PFS and uniform horizontal elongation can be differentiated at outcrop.

Weimer and Davis (1977) reported subvertical faulting in the Pierre Shale in the Denver Basin. They mapped a fault system ~800 km^2, using surface geology, borehole samples, and 2-D seismic data. They described layer-bound faulting in the Pierre Shale and recognized that the faulting occurred soon after deposition. Their observations are consistent with faulting in a PFS and were reported many years prior to the presentation of the PFS model worldwide.

Stockmal (2004) reported on the mapping of an enigmatic pop-up structure located at the leading edge of the Eastern Cordilleran deformation at Lundbreck Falls, Alberta. Here, the subhorizontal attitude of the Santonian Milk River Group lies anomalously adjacent to strata with dips more typical of Foothills structures, as reported. Stockmal (2004) noted that a possible solution to reconstruct the undisturbed geology is to interpret a back thrust in the Santonian strata. He noted that such features are rare in the Foothills. As discussed later herein, the Santonian sediments are observed to be extensively faulted in the Saskatchewan portion of the PFS.

Bishop and Williams (2000) discussed the occurrence of low conical hills at outcrop near Pueblo, Colorado, and the Black Hills of South Dakota, Montana, and Wyoming. The Campanian features occur at Pierre Shale outcrop. However, the hills (also known as Tepee Buttes, possibly named because of their conical form) are erosional remnants with limestone cores. They are thought to have been formed by warm submarine springs. The origin of the Tepee Buttes

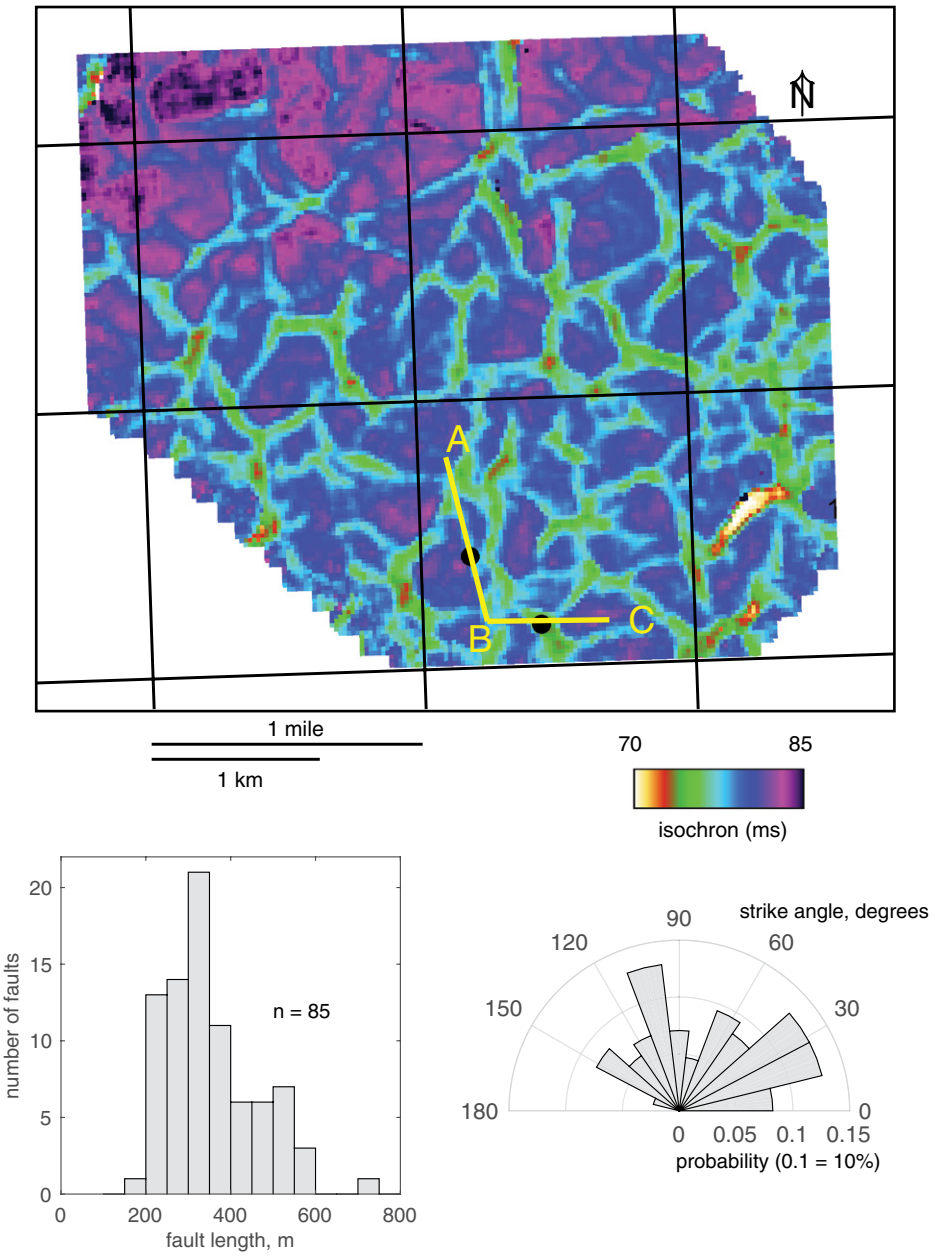

Figure 7. Coniacian Govenlock to Santonian Niobrara isochron showing a series of narrow grabens (~100 m wide on average) with variable strike direction. The average fault throw of ~7 ± 4 m is observed in the confidential wellbore BC as shown in Figure 8. The measured fault dips average 45° and range from 30° to 80° (*n = 33*).

is attributed to dewatering of underlying claystones. These features are mentioned because they are enigmatic and occur within the PFS at outcrop, as briefly discussed later herein.

DISCUSSION

Cartwright and Dewhurst (1998) outlined seven criteria for the recognition of PFS. In order of their diagnostic value, they are the observation of polygonal map-view fault patterns layer bound and delimited by stratigraphic faults, large spatial extents of up to 150,000 km^2, and faults with 10–100 m normal throw and 100 to 1000 m fault spacing. Moreover, the faulting can be divided into two or more tiers, and the fault polarity can switch. The observations presented here fulfill all criteria. However, it should be noted that the upper bound in many areas is the unconformable contact between the Late Cretaceous and the Tertiary strata. The upper bound that has been observed in other areas (Cartwright and Dewhurst, 1998) has been eroded.

The faulting imaged on the seismic data presented here is representative of the seismic database interpreted for this study. Please refer to Table 1. Older Late Cretaceous horizons (Turonian 2WS or Greenhorn) have little or no faulting. Faulting offset increases toward the ground surface, sometimes approaching 80 m. Bed dips measured in this study ranged from 22° to 80°, with most dips occurring at ~40° and 80°. These observations are consistent with those presented by Inks et al. (2010) for the Tiger Ridge pool in Montana, Gendzwill and Stauffer (2006) for an area near Saskatoon in central Saskatchewan, and Miller and Steeples (1996) for the Harlan County reservoir. The observations are also consistent with those by Sonnenberg (2013) for the Niobrara in Colorado.

The variation in the strike length and direction should be noted. The fault traces for the PFS shown in Figure 4 have no discernible strike because of their arcuate geometry. This contrasts with the linear strike lengths for the faulting shown on Figure 7. Roberts et al. (2015) used geomechanical forward modeling to investigate the evolution of PFS by interpreting the results of a finite-element model for a mud undergoing burial. Their model result for zero external stress showed faults similar to those observed on Figure 4, suggesting that this portion of the PFS occurred under zero external stress conditions. Roberts et al. (2015) also modeled PFS development in an anisotropic stress field. A small amount of anisotropy results in more linear fault strikes, more similar to the faults shown in Figure 9. Future work is planned to see if the fault strikes can be used as a paleostress indicator, as discussed by Roberts et al. (2015). This work will require a more complete database of 3-D seismic interpretations than is currently completed.

The area covered by the PFS could be extensive. As shown in Figure 2, the Pierre Shale has been mapped over 2,600,000 km^2. Do the observations presented here represent a sample set large enough to state that a Late Cretaceous PFS covers the sediments in the area? The large amount of fine-grained material deposited in the Western Interior Seaway and the extensive observations of faulting at outcrop and on borehole or seismic data seem to indicate a single PFS. Further investigation will lead to a better estimate for the PFS extent. From currently available data, it is estimated that the area encompasses over 2,000,000 km^2.

This study concentrated on mapping larger-offset faults that can be imaged on seismic data.

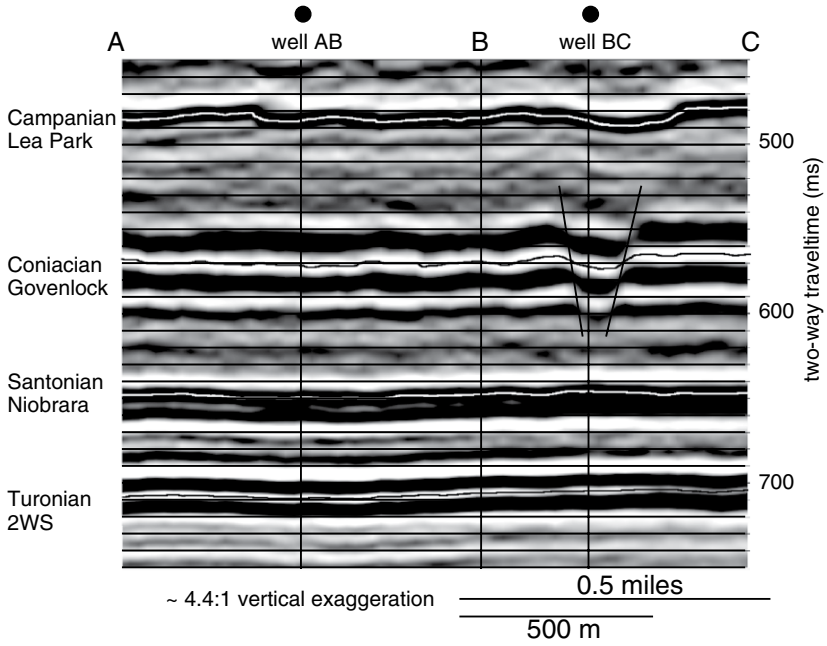

Figure 8. A north/south, then west/east seismic line showing the ~100-m-wide graben encountered in wellbore BC. The fault throw of ~7 m in the Coniacian level at the wellbore is equal to the average of 87 fault throws (7 ± 4 m) imaged by the dataset. 2WS—Second White Specked reflection.

Seismic data can only image faults if the S:N ratio allows for the reflection to be recorded from an impedance contrast that might not occur from a faulted but otherwise homogeneous rock mass. Therefore, seismic interpretations will always underestimate fault quantity. The fault densities in Table 1 suggest that a total of 25 faults/km^2 can exist within the PFS. This would imply 50 million faults with throws of 10 m or more and strike lengths on the order of 500 m. Also, myriad smaller-scale faults are observed. Consider Figures 4 and 7. There are a number of areas that appear to have structural features on the scale of 100 m length. These are fault traces. As noted by Sonnenberg and Underwood (2012), the polygonal faults scale in size. This points to the possibility of tens of millions of faults over the study area.

PFS fault blocks can be small enough in size that even densely drilled gas wells (eight wells per section; Inks et al., 2010) could miss important sealing fault traces or fault block geometries. At present, there is no commercial Late Cretaceous gas production in the east half of the study area. However, in this area, water wells are commonly drilled to 300 m depth or more for potable water. The potential that seismic data can be used to help drill water wells is currently being investigated. We are encouraging hydrocarbon exploration companies to share their seismic database with shallow-water-well drill locations to target an imaged fault.

PFS fault flow characteristics are important in the investigation of water or hydrocarbon flow in low-permeability strata (Cartwright et al., 2007; Ostanin et al., 2012). A large amount of this work could be done in the shallow gas pools in eastern Alberta and western Saskatchewan (see O'Connell, 2003), which continue down to the Tiger Ridge, Montana. These produce natural gas out of Late Cretaceous strata and are faulted with PFS geometry. Inks et al. (2010) noted that the pressures of infill wells indicated reservoir compartmentalization. However, Pierre Shale slumping at numerous areas may be indicative of open faults, if the slumping occurs at the fault traces. This is a complex problem that requires further investigation, and the large number of wellbores in the study area will greatly benefit future work.

The presence of a PFS that initiated shortly after deposition can have ramifications for the interpretation of geologic features. Stockmal (2004) summarized an extensive analysis of an outcrop in Alberta involving Late Cretaceous strata. If lithification of an in situ Late Cretaceous PFS occurred, it could have created zones of weaknesses along open faults that were subsequently involved with Cordilleran deformation. The large numbers of Santonian faults imaged in Saskatchewan (see supplementary PowerPoint P1 [see footnote 1]) suggest that a Santonian PFS at outcrop on the Cordillera could have observable PFS faulting. Because of the rarity of reported PFS faulting at outcrop, any geological work, such as provided by Stockmal (2004), should be further investigated.

Little or no faulting is observed at the ground surface. Most of the study area is covered in glacial till, Quaternary sediments, and a thin veneer of Tertiary sediments. When surface faulting is observed, this study assumed that the faulting was caused by the PFS. Unless examined and identified as PFS (such as by Maher, 2014), the areas were catalogued for future work to identify PFS. Examples of this are the fault shown in Figure 3 and the slumping at Harlan County Lake (Miller and Steeples, 1996). Future work could involve further surface mapping or seismic data interpretations, as presented here.

Stauffer and Gendzwill (1987) examined over 7320 fractures at 16 sites in Saskatchewan and Montana, measuring strike orientation in material ranging in age from the Late Cretaceous to the late Pleistocene. Most of the measurements were subvertical dips and predominant strikes of either NE/SW or NW/SE. The fault orientation was attributed to uplift that induced tensile stress and conjugate stress fractures, which were induced after fracturing parallel to the maximum horizontal stress. This model could help to explain the graben strike estimations shown of Figure 9. Stauffer and Gendzwill (1987) noted that river valleys in the area follow these directions; they suggested causality between the fractures and drainage patterns. This is another area of current research on PFS geometries and drainage patterns.

Some of the fault blocks on the seismic data had the appearance of "tilted fault blocks." This appearance is evident by quickly slicing through 3-D seismic volumes and cannot be reproduced here. However, a fault block interpretation is consistent with those observed by Inks et al. (2010) and Miller and Steeples (1996). The available seismic data volumes are being searched to provide seismic and wellbore evidence for tilted fault blocks that can be presented in an appropriate manner.

Tewksbury et al. (2014) noted that the steep dips of some of the fault planes implied host formation overpressure within a PFS. They also recognized a set of circular outcrop features they identified as fluid escape pipes. There are a number of subvertical faults in the Pierre Shale units. Also, two areas of fluid escape pipes have been identified at the Tepee Buttes in South Dakota and Colorado (Bishop and Williams, 2000; Metz, 2010). Preliminary modeling has shown that the Tepee Buttes could be imaged with seismic data

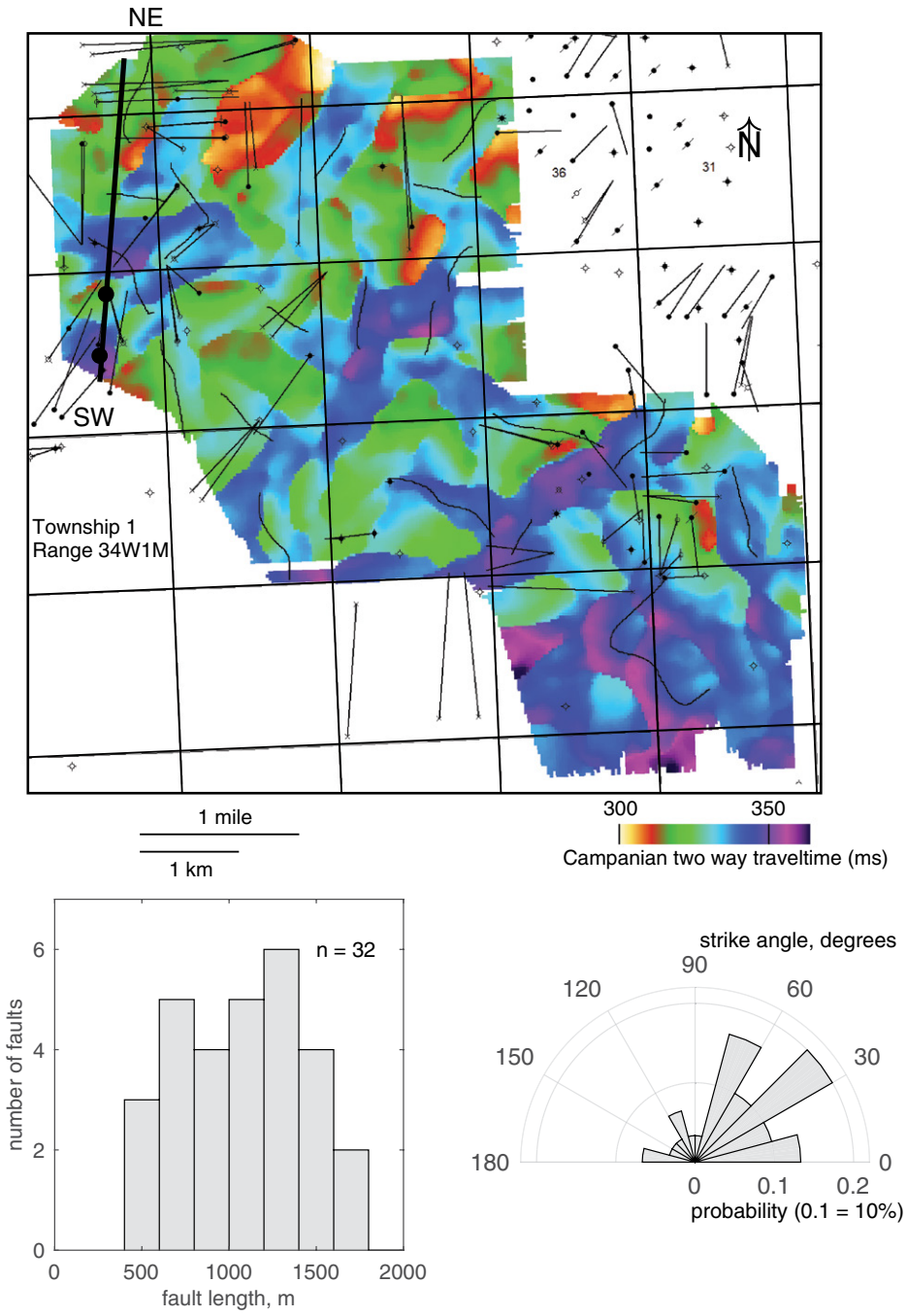

Figure 9. Map showing the Campanian Milk River reflection two-way traveltime for a three-dimensional (3-D) seismic dataset near the U.S. border in central Saskatchewan. The bin size for this dataset is 25 × 25 m. The graben edges have preferred strike directions of NE and NNE.

acquired with acquisition parameters targeting Campanian sediments at depth. The data presented here did not observe any type of circular features. However, the observation and interpretation of such features using seismic data and the extensive well database within the Great Plains PFS could help in the understanding of PFS.

IMPLICATIONS

The implications for the existence of the postulated Great Plains PFS range from surface geology interpretations to sediments at depth that have water and hydrocarbon resource potential. Pervasive slumping in the Pierre Shale at surface could indicate fault reactivation along PFS fault traces. A PFS model and subsequent fault identification could help locate shallow water wells in Saskatchewan, if the fault traces affect hydraulic conductivity. Otherwise tight hydrocarbon reservoirs could have permeability enhancement interpretations with the acquisition of 3-D seismic surveys targeting the relevant depths.

CURRENT AND FUTURE WORK

Current Work

The following work is currently under way:

(1) an analysis of PFS formation over Albian sand bodies that have compacted less than the surrounding strata to interpret if this may have affected PFS initiation;
(2) dating of the timing of a true layer-bound PFS observed in at least three locations in western Canada in Albian sediments, where the lower PFS does fault the Turonian 2WS before the initiation of the PFS presented here, using well control and 3-D seismic data;
(3) investigation of the cessation of the PFS in southern Alberta, where the amount of Upper Cretaceous coarse-grained clastics increases in thickness and lateral extent;
(4) interpretation of tilted fault blocks within the PFS;
(5) examination of outcropping faults within a 2 h drive of Calgary to identify, map, and date potential PFS faults;
(6) acquisition and interpretation of a 3-D seismic dataset to image a known area where the PFS faults appear to extend up into Cretaceous sediments within 100 m of ground surface, where the dataset would be licensed to third parties and located in an area with subsurface well control; and
(7) initial planning of a project to drill a few shallow boreholes (~300 m depth) through and away from faults identified using 3-D data for water-well production.

Future Work

Future work could include:

(1) examination of the relationship between Western Interior Seaway water salinity and the initiation of the PFS;
(2) a detailed review of 3-D seismic data to look for geological anomalies such as the Tepee Buttes and how they may be related to the PFS; and
(3) an analysis of open and closed faults by using reservoir models based upon large areas

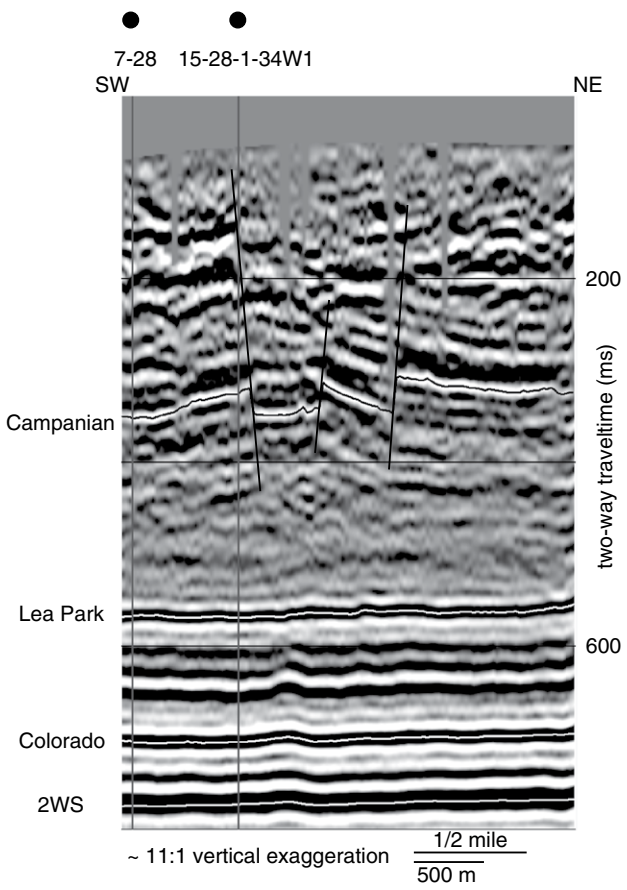

Figure 10. A southeast to northeast seismic line positioned on Figure 9 through the two wells shown in Figure 11. There is a lack of faulting below the Campanian Lea Park reflection. 2WS—Second White Specked reflection.

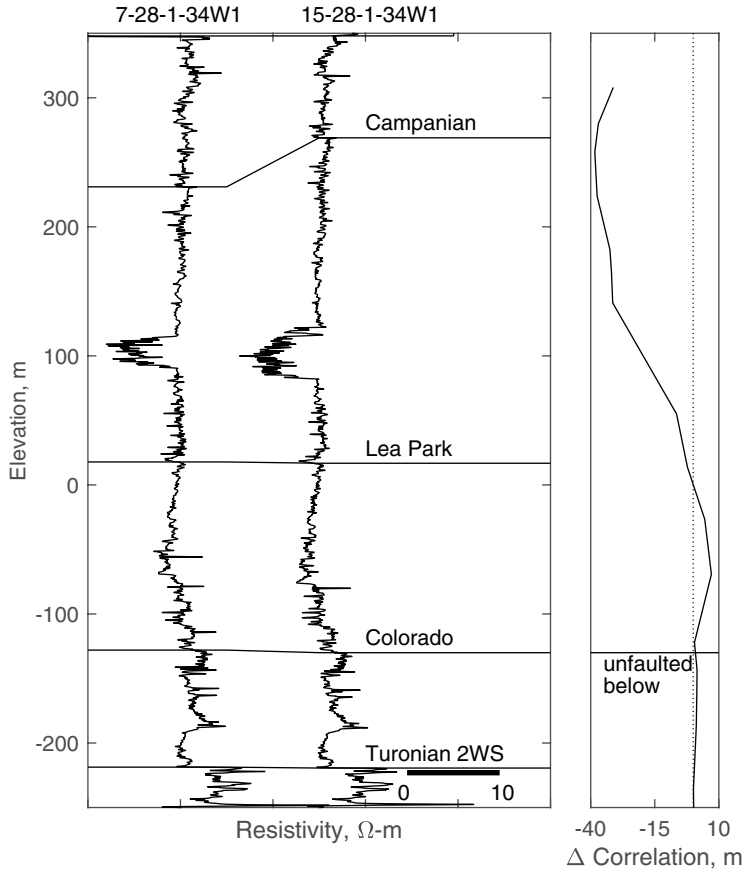

Figure 11. A two-well cross section for the two wells shown on Figure 10. There is ~40 m of structural difference in the Campanian correlation ~300 m below ground level. The Campanian Milk River correlation is 8 m lower, for a net difference of ~47 m.

of shallow biogenic gas such as Hatton/Bigstick in western Saskatchewan.

The potential application to stakeholders over a large area makes all of the current and future work worthwhile.

CONCLUSIONS

This paper has investigated the idea that fine-grained sediments in the Late Cretaceous Western Interior Seaway of North America formed a PFS. A number of seismic lines and datasets image fracturing consistent with the definition of a PFS. This fracturing has been observed by others, helping to confirm the presence of a PFS. The recognition and acceptance of the Great Plains PFS will help to interpret the morphology for this area. The large numbers of wellbore and outcrop locations will help in the interpretation of PFS mapped in other areas. A specific example would be the examination of open or closed faults, as this is an important consideration for hydrocarbon migration and entrapment. It is hoped than an immediate benefit of this work will be enhanced water-well drilling in arid locations.

ACKNOWLEDGMENTS

I thank John Waldron of the University of Alberta, who freely shared his knowledge, and Agi Pawlak and Peter St-Onge, who provided important suggestions and edits to the manuscript.

REFERENCES CITED

Bamburak, J., and Nicolas, M., 2010, Upper Cretaceous Stratigraphy of the Pembina Hills Area: Manitoba Geological Survey Field Trip Guide Book: http://www.manitoba.ca/iem/geo/mgstracker/images/region6/2010_fieldtrip.pdf (accessed November 2016).

Bertog, J., 2010, Stratigraphy of the lower Pierre Shale (Campanian): Implications for the tectonic and eustatic controls on facies distributions: Journal of Geological Research, v. 2010, 910243, doi:10.1155/2010/910243.

Bishop, G., and Williams, A., 2000, Fossil crabs from Tepee Buttes, submarine seeps of the Late Cretaceous Pierre Shale, South Dakota and Colorado, U.S.A.: Journal of Crustacean Biology, v. 20, no. 2, p. 286–300, doi:10.1163/1937240X-90000031 (accessed November 2016).

Blakey, R., 2014. Paleogeography and Geologic Evolution of North America: Arizona, USA: http://cpgeosystems.com/nam.html (accessed November 2016).

Brinker, J., and Scherer, G., 1990, Sol-Gel Science: The Physics and Chemistry of Sol-Gel Processing: San Diego, Academic Press, 908 p.

Caldwell, W., 1968, The Late Cretaceous Bearpaw Formation in the South Saskatchewan River Valley: Saskatchewan Research Council Geology Division Report 8, https://www.wsask.ca/PageFiles/2978/The%20Late%20Cretaceous%20Bearpaw%20Formation%20in%20the%20South%20Saskatchewan%20River%20Valley,%201968,%20Caldwell,%20W.G.E.,%20SRC%20Geology%20Division%20Report%20No.%208,%20C.06.Z-16.pdf (accessed November 2016).

Carruthers, D., Cartwright, J., Jackson, M., and Schutjens, P., 2013, Origin and timing of layer-bound radial faulting around North Sea salt stocks: New insight into the evolving stress state around rising diapirs: Marine and Petroleum Geology, v. 48, p. 130–148, doi:10.1016/j.marpetgeo.2013.08.001.

Cartwright, J., 2011, Diagenetically induced shear failure of fine-grained sediments and the development of polygonal fault systems: Marine and Petroleum Ge-

TABLE 1. SUMMARY POLYGONAL FAULT SYSTEM (PFS) OBSERVATIONS FOR THIS STUDY

Period			Age	Picks (Ma)	Elevation at Alida, Sask. (m)	PFS comments	PFS fault characteristics					Comments
							Throw (m)	Strike	Dip angle (°)	Length (m)	Fault density (faults/km^2)	
Quaternary					600							Outcrop. Flat surface topography with ~10 m valley incisions.
			Pleistocene	2.6	550							Can use water wells for data points (www.wsask.ca)
Tertiary			Paleocene	65		The upper bound is at base Tertiary for the observations presented here						
Late Cretaceous			Maastrichtian		500							Borehole imaging begins (logging below surface casing)
	Pierre Shale	Bearpaw, Milk River, Belly River	Campanian	72.1		Up to 80 m offset observed in Saskatchewan but not presented here						
					380		Max 80					Indications of tilted fault blocks (not shown here)
				74.7			30 ± 15	Directional	22–80	100–1500	~5	Upper Campanian generally has less faulting than the Lower Campanian
					275	Less faults but more vertical throw; see Figure 7						Somewhat connected faulting
					200							Seismic data imaging begins for typical acquisition parameters
				79?	150		20 ± 10	Directional	30–80	Up to 1500	~10	
				83.6								The entire Late Cretaceous appears to be a single tier of deformation
			Santonian									
	Colorado Group	Niobrara		86.3	75	Pervasive faulting; see Figure 10	10 ± 10	Random	30–80	200 to 800	~10	Connected polygonal faults
			Coniacian	89.8	25							
			Turonian									Predominantly mudstones and shales above
												Rare, disconnected faulting
		2WS		93.9	–50	PFS begins	Up to 2	Random	50	Up to 500	<<1	The Turonian Second White Speckled Shale (2WS) is a siliciclastic interval
			Cenomanian	100								

Note: Adopted somewhat from St-Onge (2016). Depth are taken from vertical well control located at 49.4526°N, 101.8186°W. 2WS—Second White Specked Shale.

ology, v. 28, p. 1593–1610, doi:10.1016/j.marpetgeo.2011.06.004.

Cartwright, J., 2014, Are outcrop studies the key to understanding the origins of polygonal fault systems?: Geology, v. 42, no. 6, p. 559–560, doi:10.1130/focus062014.1.

Cartwright, J., and Dewhurst, D., 1998, Layer-bound compaction faults in fine-grained sediments: Geological Society of America Bulletin, v. 110, no. 10, p. 1242–1257, doi:10.1130/0016-7606(1998)110<1242:LBCFIF>2.3.CO;2.

Cartwright, J., and Lonergan, L., 1996, Volumetric contraction during the compaction of mudrocks: A mechanism for the development of regional-scale polygonal fault systems: Basin Research, v. 8, p. 183–193, doi:10.1046/j.1365-2117.1996.01536.x.

Cartwright, J., Huuse, M., and Aplin, A., 2007, Seal bypass systems: American Association of Petroleum Geologists Bulletin, v. 91, no. 8, p. 1141–1166, doi:10.1306/04090705181.

Christopher, J.E., Yurkowski, M., Nicolas, M., and Bamburak, J., 2006, The Cenomanian–Santonian Colorado formations of eastern southern Saskatchewan and southwestern Manitoba, *in* Gilboy, C.F., and Whittaker, S.G., eds., Saskatchewan and Northern Plains Oil & Gas Symposium 2006: Saskatchewan Geological Society Special Publication 19, p. 299–318.

Dewhurst, D., Cartwright, J., and Lonergan, L., 1999, Three-dimensional consolidation of fine-grained sediments: Canadian Geotechnical Journal, v. 36, p. 355–362, doi:10.1139/t98-101.

Dyman, T., Cobban, W., Fox, J., Hammond, R., Nichols, D., Perry, W., Jr., Porter, K., Rice, D., Setterholm, D., Shurr, G., Tysdal, R., Haley, J., and Campen, E., 1994, Cretaceous rocks from southwestern Montana to southwestern Minnesota, northern Rocky Mountains, and Great Plains, *in* Shurr, G.W., Ludvigson, G.A., and Hammond, R.H., eds., Perspectives on the Eastern Margin of the Cretaceous Western Interior Basin: Geological Society of America Special Paper 287, p. 5–26, doi:10.1130/SPE287-p5.

Gay, A., Lopez, M., Cochonat, P., and Sermondadaz, G., 2004, Polygonal faults-furrows system related to early stages of compaction—Upper Miocene to recent sediments of the Lower Congo Basin: Basin Research, v. 16, p. 101–116, doi:10.1111/j.1365-2117.2003.00224.x.

Gendzwill, D., and Stauffer, M., 2006, Shallow faults, Upper Cretaceous clinoforms, and the Colonsay collapse, Saskatchewan: Canadian Journal of Earth Sciences, v. 43, no. 12, p. 1859–1875, doi:10.1139/e06-071.

Gill, J., and Cobban, W., 1965, Stratigraphy of the Pierre Shale, Valley City and Pembina Mountain Areas North Dakota: U.S. Geological Survey Professional Paper 392-A, 20 p.

Goulty, N., 2001, Mechanics of layer-bound polygonal faulting in fine-grained sediments: Journal of the Geological Society of London, v. 159, p. 239–246, doi:10.1144/0016-764901-111.

Goulty, N., and Swarbrick, R., 2005, Development of polygonal fault systems: A test of hypotheses: Journal of the Geological Society of London, v. 162, p. 587–590, doi:10.1144/0016-764905-004.

Henriet, J.P., Batist, M., and Verschuren, M., 1991, Early fracturing of Paleogene clays, southernmost North Sea: Relevance to mechanisms of primary hydrocarbon migration, *in* Spenser A.M., ed., Generation, Accumulation and Production of Europe's Hydrocarbons: European Association of Petroleum Geologists Special Publication 1, p. 217–227.

Inks, T., Baclawski, P., Seaton, C., and Estes, S., 2010, Productive wrench grabens imaged on 3D seismic, Tiger Ridge Field, Blaine and Hill Counties, Montana: American Association of Petroleum Geologists Search and Discovery Article 20083, 8 p.

Ishii, E., Funaki, H., Tokiwa, T., and Ota, K., 2010, Relationship between fault growth mechanism and permeability variations with depth of siliceous mudstones in northern Hokkaido, Japan: Journal of Structural Geology, v. 32, no. 11, p. 1792–1805, doi:10.1016/j.jsg.2009.10.012.

Jackson, C., Carruthers, D., Mahlo, S., and Briggs, O., 2014, Can polygonal faults help locate deep-water reservoirs?: America Association of Petroleum Geologists Bulletin, v. 98, no. 9, p. 1717–1738, doi:10.1306/03131413104.

Lopez, T., Antoine, R., Darrozes, J., Rabinowicz, M., and Baratoux, D., 2015, Formation of polygonal fracture system as a result of hydrodynamic instabilities in clay-rich deposits: Geological Society of America Abstracts with Programs, v. 47, no. 7, p. 324.

Maher, H.D., 2014, Distributed normal faults in the Niobrara Chalk and Pierre Shale of the central Great Plains of the United States: Lithosphere, v. 6, no. 5, p. 319–334, doi:10.1130/L367.1.

Maher, H.D., Ferguson, S., Korth, R., Marshall, J., and Pickett, L., 2015, Strata bound vein array in the Pierre Shale, Lake Francis Case, South Dakota, U.S.A.: Rocky Mountain Geology, v. 50, no. 2, p. 153–165, doi:10.2113/gsrocky.50.2.153.

Metz, C., 2010, Tectonic controls on the genesis and distribution of Late Cretaceous, Western Interior Basin hydrocarbon-seep mounds (Tepee Buttes) of North America: The Journal of Geology, v. 118, p. 201–213, doi:10.1086/650181.

Miller, R., and Steeples, D., 1996, Evaluation of Fault Scarp at Harlan County Lake, Harlan County, Nebraska, Using High Resolution Seismic Reflection Surveying: Kansas Geological Survey Open-File Report 96-32, http://www.kgs.ku.edu/Geophysics/Reports2/HarlanCo.pdf (accessed November 2016).

Ostanin, I., Anka, Z., and di Primio, R., 2012, Identification of a large Upper Cretaceous polygonal fault network in the Hammerfest basin: Implications on the reactivation of regional faulting and gas leakage dynamics, SW Barents Sea: Marine Geology, v. 332–334, p. 109–125, doi:10.1016/j.margeo.2012.03.005.

Roberts, D., Crook, A., Cartwright, J., and Profit, M., 2015, Investigating the Evolution of Polygonal Fault Systems Using Geomechanical Forward Modeling, *in* 49th U.S. Rock Mechanics/Geomechanics Symposium held in San Francisco, CA, 28 June–1 July.

Roberts, L., and Kirschbaum, M., 1995, Paleogeography of the Late Cretaceous of the Western Interior of Middle North America—Coal Distribution and Sediment Accumulation: U.S. Geological Survey Professional Paper 1561, 115 p., http://pubs.usgs.gov/pp/1561/report.pdf (accessed November 2016).

Schröder-Adams, C.J., Cumbaa, S.L., Bloch, J., Leckie, D.A., Craig, J., Seif El-Dein, S.A., Simons, D.-J.H., and Kenig, F., 2001, Late Cretaceous (Cenomanian to Campanian) paleoenvironmental history of the eastern Canadian margin of the Western Interior Seaway: Bonebeds and anoxic events: Palaeogeography, Palaeoclimatology, Palaeoecology, v. 170, p. 261–289, doi:10.1016/S0031-0182(01)00259-0.

Schultz, L., Tourtelot, H., Gill, J., and Boerngen, J., 1980, Composition and Properties of the Pierre Shale and Equivalent Rocks, Northern Great Plains Region: U.S. Geological Survey Professional Paper 1064, 123 p., http://pubs.usgs.gov/pp/1064b/report.pdf (accessed November 2016).

Slingerland, R., Kump, L., Arthur, M., Fawcett, P., Sageman, B., and Barron, E., 1996, Estuarine circulation in the Turonian Interior Seaway of North America: Geological Society of America Bulletin, v. 108, no. 8, p. 941–952 doi:10.1130/0016-7606(1996)108<0941:ECITTW>2.3.CO;2.

Sonnenberg, S., 2013, New reserves in an old field, the Niobrara resource play in the Wattenberg Field, Denver Basin, Colorado: Denver, Colorado, Unconventional Resources Technology Conference, 12–14 August, doi:10.1190/URTEC2013-098.

Sonnenberg, S., and Underwood, D., 2012, Polygonal fault systems: A new structural style for the Niobrara Formation, Denver Basin, Colorado: America Association of Petroleum Geologists Search and Discovery Article 50624, http://www.searchanddiscovery.com/documents/2012/50624sonnenberg/ndx_sonnenberg.pdf (accessed November 2016).

St-Onge, A., 2016, Interpretation of the Late Cretaceous polygonal fault system at Alida, Saskatchewan: Geological Society of America Abstracts with Programs, v. 48, no. 7, doi:10.1130/abs/2016AM-287005

Stauffer, M., and Gendzwill, D., 1987, Fractures in the Northern Plains, stream patterns, and the midcontinent stress field: Canadian Journal of Earth Sciences, v. 24, p. 1086–1097, doi:10.1139/e87-106.

Stockmal, G., 2004, A pop-up structure exposed in the outer Foothills, Crowsnest Pass area, Alberta: Bulletin of Canadian Petroleum Geology, v. 52, no. 2, p. 139–155, doi:10.2113/52.2.139.

Stoffer, P., 2003, Geology of the Badlands National Park: A Preliminary Report: U.S. Geological Survey Open File Report 03-35, 65 p., http://3dparks.wr.usgs.gov/badl/images/of03-35.pdf (accessed November 2016).

Tewksbury, B., Hogan, J., Kattenhorn, S., Mehrtens, C., and Tarabees, E., 2014, Polygonal faults in chalk: Insights from extensive exposures of the Khoman Formation, Western Desert, Egypt: Geology, v. 42, no. 6, p. 479–482, doi:10.1130/G35362.1.

Watterson, J., Walsh, J.J., Nicol, A., Nell, P.A.R., and Bretan, P.G., 2000, Geometry and origin of a polygonal fault system: Journal of the Geological Society of London, v. 157, p. 151–162, doi:10.1.1.112.5134.

Weimer, R., 1960, Upper Cretaceous stratigraphy, Rocky Mountain area: America Association of Petroleum Geologists Bulletin, v. 44, p. 1–20.

Weimer, R., and Davis, T., 1977, Stratigraphic and seismic evidence for Late Cretaceous growth faulting, Denver Basin, Colorado, *in* Payton, C., ed., Seismic Stratigraphy—Applications to Hydrocarbon Exploration: America Association of Petroleum Geologists Memoir 26, p. 277–299, doi:10.1306/M26490C17.

Zhang, L., and Buatois, L.A., 2014, Sedimentary facies and depositional environments of the Upper Devonian–Lower Mississippian Bakken Formation in eastern Saskatchewan, *in* Summary of Investigations 2014, Volume 1, Saskatchewan Geological Survey, Sask: Ministry of the Economy Miscellaneous Report 2014-4.1, Paper A-3, 18 p., http://publications.gov.sk.ca/documents/310/91969-A-3%20Zhang%20and%20Buatois.pdf (accessed November 2016).

Science Editor: David I. Schofield
Associate Editor: Nicholas Erik Timms

Manuscript Received 23 May 2016
Revised Manuscript Received 28 October 2016
Manuscript Accepted 4 December 2016

Printed in the USA